Available online at www.sciencedirect.com
SCIENCE DIRECT
Physica C 437–438 (2006) 171–175
PHYSICA C
www.elsevier.com/locate/physc

Anomalous flux dynamics in magnesium diboride films

M.N. Kunchur [a,*], G. Saracila [a], D.A. Arcos [a], Y. Cui [b], A. Pogrebnyakov [b], P. Orgiani [b], X.X. Xi [b], P.W. Adams [c], D.P. Young [c]

[a] Department of Physics and Astronomy, University of South Carolina, Columbia, SC 29208, United States
[b] Department of Physics, Department of Materials Science and Engineering, The Pennsylvania State University, PA 16802, United States
[c] Department of Physics and Astronomy, Louisiana State University, Baton Rouge, LA 70803, United States

Available online 7 February 2006

Abstract

The flux dynamics in magnesium diboride films becomes altered by scattering resulting in an unprecedented quenching of flux motion that is beyond conventional vortex pinning. At currents approaching the pair-breaking value and magnetic fields approaching the upper-critical field, the conductance diverges and the current-resistance and temperature–conductance curves become parallel, showing mainly a shift in the transition due to pair-breaking with minimal signs of flux motion.

PACS: 74.25.Op; 74.25.Fy; 74.70.Ad; 74.25.Qt; 74.25.Sv

Keywords: Superconductor; Superconductivity; Vortex; Vortices; Flux

1. Background

In a type-II superconductor, an applied flux density B or current I has two effects. First the superconductivity is suppressed and the transition temperature T_c shifts downward in the manner [1–3]: $T_c(B,I) \approx T_c(0,0) - B|dT/dH_{c2}| - I^{2/3}|dT/dI_d^{2/3}|$, where H_{c2} is the upper critical field and I_d is the depairing or pair-breaking critical current; the slopes are evaluated at $T_c(0,0)$.

The second effect of B and I is that they both broaden the conductance versus temperature $G(T)$ transition. The current produces a self magnetic field which causes the local T_c to decrease with the distance from the center due to Silsbee's mechanism [2]. Additionally, variations in sample cross section cause the local current density and hence the local T_c to vary. Note that for very low-value currents $I \ll I_d$—as are typically used—the transition will not be broadened; in this work we use substantial currents $I \sim I_d(T)$.

Similarly, an applied magnetic field broadens $G(T)$, because of flux motion, and limits the maximum G to a finite value given by [2,4]: $G_f \sim G_n H_{c2}/B$. This $G_f \propto 1/B$ field dependence persists even in the case of highly driven non-linear and unstable flux flow [5,6].

Fig. 1(a) shows an example of this expected behavior in the $MgCNi_3$ system: B causes both a shift and a progressive broadening. These measurements were conducted at a high current density ($j = 2 \times 10^5$ A/cm^2) so that the flux motion induced resistance did not freeze out quickly as the temperature is lowered. Notice that the broadening with B is more conspicuous when the curves are plotted as G vs T (inset) rather than R vs T. If on the other hand $R(T)$ is measured at currents too low to overcome pinning, then the $R(T)$ curves in different B will appear parallel. This is seen in Fig. 1(b). The vast majority of published transport measurements lie in this regime; they are carried out with feeble currents below the depinning threshold I_c, so that broadening with B is prevented by flux pinning. These represent trivial cases where $R(T)$ curves in different B may appear to be parallel. Note that even in this low-I case, when the same data is plotted as $G(T)$ (inset of Fig. 1(b)) there is a noticeable divergence between curves at different B.

* Corresponding author. Fax: +1 803 777 3065.
E-mail address: kunchur@sc.edu (M.N. Kunchur).

0921-4534/$ - see front matter © 2005 Elsevier B.V. All rights reserved.
doi:10.1016/j.physc.2005.12.028

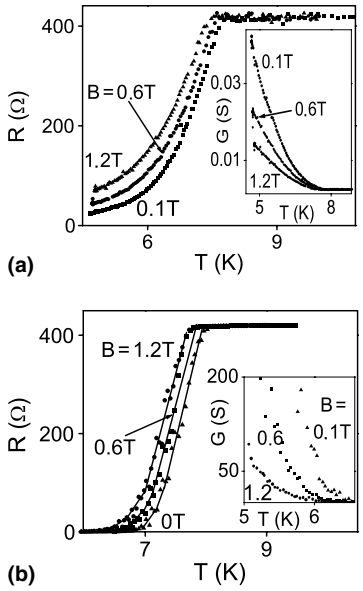

Fig. 1. (a) $R(T)$ curves of a $MgCNi_3$ film at a high value of j ($=2\times10^5$ A/cm^2) in different indicated flux densities; inset shows the same data plotted as conductance. (b) Similar set of $R(T)$ curves at a very low j ($=264$ A/cm^2); lines are guides to the eye. Inset shows corresponding $G(T)$ curves.

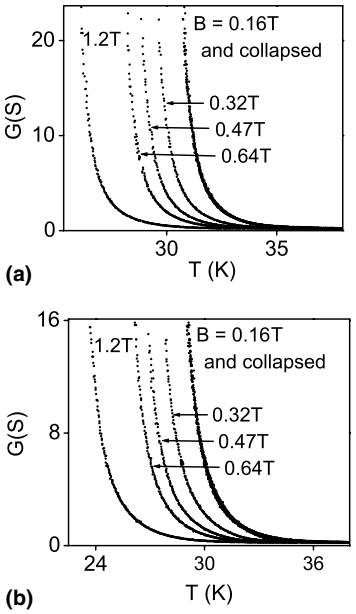

Fig. 2. $G(T)$ curves for a postannealed MgB_2 film at different values of B (left to right: 1.2, 0.64, 0.47, 0.32, and 0.16 T). (a) Curves at $I=8.7$ mA ($j\approx7\times10^5$ A/cm^2). (b) $I=15.6$ mA ($j\approx1.3\times10^6$ A/cm^2). For both panels, the rightmost curve represents the collapse of all five fields.

The dividing line between the two types of behavior is the value of I relative to I_c. Typically I_c is significantly lower than I_d and has a maximum value for columnar defects whose size, orientation, and distribution match the vortex lattice. As discussed elsewhere [7], the maximum value of I_c does not exceed $I_{c,max}\sim0.16I_d$ for the highest pinning. In this work even when I well exceeds this limit, the response still shows a lack of significant flux motion.

2. Results

Fig. 2 shows $G(T)$ curves at different B measured on MgB_2 films with built in disorder (these films are c-axis oriented but not epitaxial, and have H_{c2} and normal resistivities several times higher than single-crystal values [8]). In stark contrast to the $MgCNi_3$, the $G(T)$ curves at different B have identical shapes and show essentially no B dependent broadening; when shifted horizontally they collapse together. Also the $G(T)$ transition widths are abnormally narrow considering the high values of j, and the conductance is abnormally high (i.e., the flux motion induced voltage vanishes). As shown elsewhere [7,9,10], at the point where the resistance is vanishing and flux motion is freezing out we have $I\sim I_d(T)/2$, thus making a conventional pinning mechanism unlikely in light of the earlier discussion regarding the limit $I_c<0.16I_d$. Also a conventional pinning mechanism would require a substantial fraction of the sample to be filled by an impurity phase. This is impossible in light of the known purity of the sample. Note that problems with sample quality, I or B inhomogeneity, or other experimental artifacts would have just the opposite effect and would show instead the lack of a universal collapse, broader transitions, and a lower conductance, which is the opposite of what is observed.

This anomaly of B independent shapes of $R(T)$ and $G(T)$ curves near T_c, is also reflected in I vs V curves at fixed temperatures. Fig. 3(a) shows an example of transport characteristics at low temperatures and high fields; other sets of curves under different conditions have been presented else-

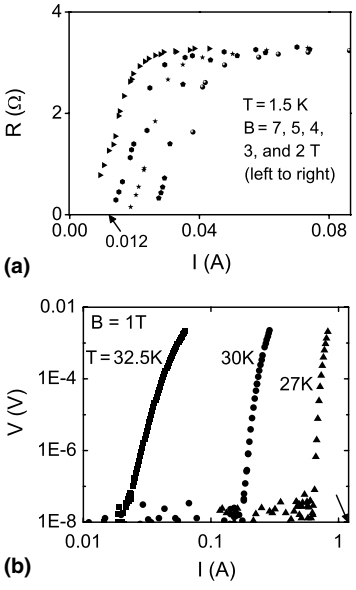

Fig. 3. (a) $R(I)$ curves for a postannealed MgB_2 film at $T\approx0$ (i.e., $T\ll T_c$) at different B values. (b) $V(I)$ curves on another postannealed MgB_2 film showing the very low end of dissipation (data from ORNL [11]). For both panels the arrows point to the current value for which $j\approx1$ MA/cm^2.

where [8,10]. Once again there is virtually no evidence of flux motion—the curves at different B are parallel and do not become progressively broader with increasing B but only shift because of the B dependent suppression of I_d. Also the curves are abnormally steep—the (extrapolated) onset of dissipation again corresponds to $I \sim I_d(T)/2$. This behavior has also been observed by other groups and Fig. 3(b) shows data [11] from the Oak Ridge National Laboratory (ORNL). Their measurements are carried out with higher voltage sensitivity. Notice that the slopes are extremely steep and correspond to "n values" in the ~100 range (the n value is defined as the exponent in the power law $E \propto j^n$ exhibited by the transport characteristic as E vanishes). Their transport measurements agree with their measured flux creep rate S (which should go as $S = 1/[n-1]$) obtained from magnetic relaxation. These unprecedented n values imply the same drastic suppression of flux motion at the very low end ($I \to 0$) of the driving force scale as we have observed at the extreme high end ($I \to I_d$).

In order to shed more light on the possible causes of the severe braking of flux motion, we investigated the transport response in the limit of very low B values. These data are shown in Fig. 4. Curiously, the curve shapes change at low B, indicative of flux motion, but become steep and parallel above ~0.1 T. Normally flux moves more easily at large B and not the other way around. This cross-over field of $H_x \sim 0.1$ T corresponds to the value above which the gap in the π band is suppressed and the two-band superconducting state of MgB_2 reverts to one where mainly the σ band contributes. This has been established by STM based tunneling measurements [12] and through specific heat behavior [13]. Could it be that the now normal or gapless π band provides an alternative low-dissipation path shorting out the σ-band mixed state? The π band in these films is in fact much cleaner than σ as inferred from the shape of $H_{c2}(T)$ near T_c using the Gurevich theory [14]. It turns out that impurity scattering affects the diffusivities of the two bands unequally. If unequal diffusivities are at the root of the anomalous flux dynamics, a sufficiently clean MgB_2 sample should exhibit conventional flux dynamics. In this clean limit many other properties, such as the T dependence of H_{c2}, also become conventional [14].

With this in mind, we studied films of MgB_2 made by the HPCVD in situ process where the disorder can be progressively increased by carbon doping. For the undoped case this leads to extremely clean epitaxial films whereas the doped films are uniaxial. The resulting IV transport characteristics are shown in Fig. 5. Panel (a) shows raw data on a pure sample. The curves shapes are not parallel but depend on B as per conventional flux dynamics. When V is divided by B, the curves become parallel and can be shifted horizontally and made to collapse as shown in panel (b). On the other hand panel (c) shows a film that is 22 at. % carbon doped (also made by the HPCVD process). Here again we see the anomalous dependence on B where the I–V curves become parallel (without division by B). The pure and carbon-doped films show a corresponding difference

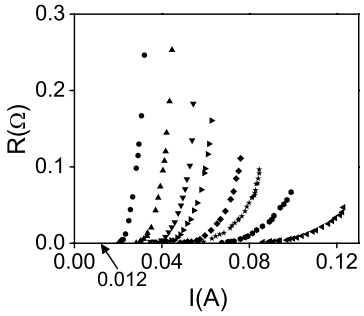

Fig. 4. $R(I)$ curves at $T = 20$ K ($\approx T_c/2$) for a postannealed MgB_2 film. From left to right, $B = 1.2$, 0.6, 0.3, 0.2, 0.11, 0.08, 0.06, and 0.033 T; normalized range: $B/H_{c2}(T) \sim 0.4\%$ –16%. The curves at very low fields show the usual field dependent broadening, while at higher B they become unexpectedly steep and parallel, signaling the freezing of flux motion. The arrow points to the I for which $j \approx 1$ MA/cm^2.

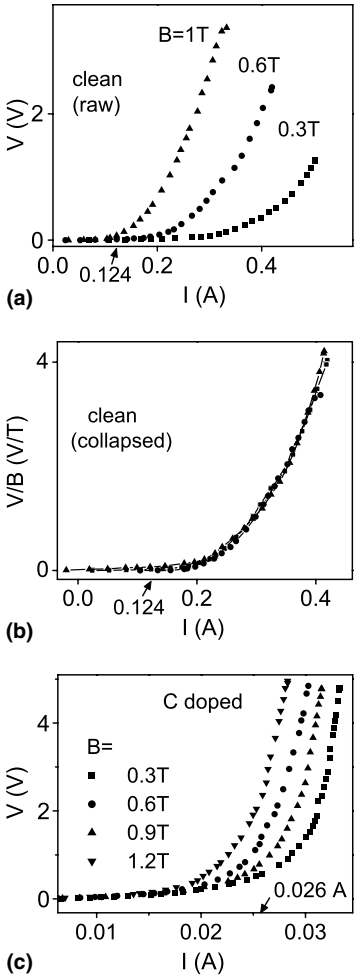

Fig. 5. (a) $V(I)$ curves for a clean HPCVD in situ epitaxial MgB_2 film showing conventional B dependent ($V \propto B$) broadening due to flux motion. $T = 10$ K. (b) Above V values divided by B and then shifted horizontally and made to collapse. (c) $V(I)$ curves for a carbon-doped HPCVD in situ MgB_2 film. $T = 6$ K. The arrows point to the I values for which $j \approx 1$ MA/cm^2.

in their $H_{c2}(T)$ functions, changing from a conventional shape to one indicative of disparate diffusivities in the two bands [15].

3. Discussion and conclusions

The dynamics of flux vortices in disordered MgB_2 shows an interesting regime where their motion is drastically suppressed and the system behaves like a highly conducting normal conductor or a type I superconductor. The $R(T)$ curves near T_c (Fig. 2) and the $R(I)$ curves at all temperatures (Fig. 3(a)) shift with B through its pair-breaking action (i.e., suppression of T_c or I_d) but without much broadening or change in shape with B. This is uncharacteristic of any type or regime of flux motion. The same surprising reluctance of flux motion is also evident in magnetic relaxation where the relaxation rates are abnormally slow and the corresponding n values are abnormally large [11]. There is a third kind of probe that also fails to see flux motion in disordered MgB_2 films but sees it in single crystals. This probe consists of parking a scanning-tunneling microscope tip at a fixed point and sensing flux motion through temporal variations in differential conductance [16].

The regime with anomalous flux dynamics is not a narrow one but rather includes most of the phase space ($T \sim 0$ to T_c and $B \sim 0.1$ to H_{c2}). It seems to correspond to the situation when impurity scattering affects the π and σ diffusivities unequally and when B is large enough to mostly extinguish the weaker π gap. In this regime, H_{c2} has the unconventional temperature dependence indicative of a cleaner π band. Thus the π band now behaves like a highly conductive normal conductor in parallel with the mixed state of the σ band.

The situation is analogous to having a thin superconducting film deposited onto a thick silver substrate. In this case the resistance remains zero as long as $I < I_c(B)$. Once I_c is exceeded, the mixed state resistance of the superconductor exceeds that of the substrate, and the latter then carries most of the current. The I–V curve then reflects the (very low) resistance of the substrate, which is not B dependent, leading to parallel curves that merely shift with B. Looking at this from another point of view, the conduction through the silver boosts the viscous drag felt by the vortices. The generation of the local electric field within the vortex core and its vicinity arises from the acceleration of superfluid (Bardeen–Stephen mechanism) and the relaxation of the order parameter (Tinkham mechanism) [2]. The silver does not contribute to the generation of electric field but does add to the conductance and eddy-current damping, thus boosting the viscous drag coefficient. In this scenario, the layers of silver closest to the interface will feel the largest modulation of B and hence contribute the most to the damping. In MgB_2, the π band spatially coexists with the vortex structure and hence provides a more exaggerated effect than the silver analogy. Besides the effect on viscosity, there may be some novel mechanism related to this two-band scenario that leads to a giant enhancement of pinning. We hope the results presented here will generate theoretical activity leading to a complete solution.

4. Experimental methods

The samples of Fig. 1 are polycrystalline $MgCNi_3$ films on sapphire substrates [17] with bridge dimensions $t \approx 20$ nm, $w \approx 250$ μm, and $l \approx 2$ mm.

The samples of Figs. 2–4 are uniaxially (c-axis perpendicular to substrate) oriented MgB_2 films on sapphire grown by depositing B on sapphire and subsequently annealing in Mg vapour [11,18,19]. The bridge dimensions were $t \approx 400$ nm, $w \approx 3$ μm, and $l \approx 60$ μm, except for the data of Fig. 3(b), which has bridge dimensions $t \approx 600$ nm, $w \approx 200$ μm, and $l \approx 3$ mm.

The MgB_2 films on SiC substrates of Fig. 5 were grown by a hybrid physical–chemical vapour deposition (HPCVD) in situ process [15]. The bridge dimensions in this case are $t \approx 190$ nm, $w \approx 65$ μm, and $l \approx 3.5$ mm for the clean and $t \approx 170$ nm, $w \approx 15$ μm, and $l \approx 800$ μm for the doped films, respectively. Further details about the sample preparation and characterization is given in the cited references [15,17–19].

The electrical conductance was measured with a continuous DC source for currents below 50 μA and with a pulsed current source for higher currents. A detailed description of the pulsed measurement technique is provided in our previous review articles [1,9].

Acknowledgements

We would like to acknowledge useful discussions with A. Gurevich, B.I. Ivlev, J.M. Knight, D.K. Christen, F. Nori, S. Savelev, V.L. Kogan, J.R. Clem, and M.R. Eskildsen. We would like to thank S.I. Lee for providing samples used in the earlier work [8,20], some of which were repatterned for further measurements. The data for Fig. 3(b) were provided by C. Cantoni, D.K. Christen, and J.R. Thompson [11]. Support was provided by the US Department of Energy through grant number DE-FG02-99ER45763.

References

[1] M.N. Kunchur, Mod. Phys. Lett. B. 9 (1995) 399.
[2] M. Tinkham, Introduction to Superconductivity, 2nd ed., McGraw Hill, New York, 1996.
[3] M.N. Kunchur, D.K. Christen, C.E. Klabunde, J.M. Phillips, Phys. Rev. Lett. 72 (1994) 752.
[4] A.I. Larkin, Yu.N. Ovchinnikov, in: D.N. Langenberg, A.I. Larkin (Eds.), Nonequilibrium Superconductivity, Elsevier, Amsterdam, 1986, Chapter 11.
[5] A.I. Larkin, Yu.N. Ovchinnikov, Zh. Eksp. Teor. Fiz. 68 (1975) 1915 [Sov. Phys. JETP 41, 960 (1976)].
[6] M.N. Kunchur, Phys. Rev. Lett. 89 (2002) 137005.
[7] D.H. Arcos, M.N. Kunchur, Phys. Rev. B 71 (2005) 184516.
[8] M.N. Kunchur, C. Wu, D.H. Arcos, B.I. Ivlev, S.I. Lee, W.N. Kang, Phys. Rev. B 68 (2003) 100503.

[9] M.N. Kunchur, Top. Rev. J. Phys: Condens. Matter 16 (2004) R1183.
[10] M.N. Kunchur, C. Wu, D.H. Arcos, G. Saracila, E.-M. Choi, K.H.P. Kim, W.N. Kang, S.-I. Lee, Braz. J. Phys. 33 (2003) 705.
[11] J.R. Thompson et al., Supercond. Sci. Technol. 18 (2005) 970.
[12] M.R. Eskildsen et al., Phys. Rev. Lett. 89 (2002) 187003; M.R. Eskildsen et al., Physica C 385 (2003) 169.
[13] F. Bouquet et al., Phys. Rev. Lett. 89 (2002) 257001.
[14] A. Gurevich, Phys. Rev. B 67 (2003) 184515.
[15] A.V. Pogrebnyakov et al., Appl. Phys. Lett. 85 (2004) 2017.
[16] A. Kohen et al., Appl. Phys. Lett. 86 (2005) 212503.
[17] D.P. Young et al., Phys. Rev. B 68 (2003) 020501.
[18] W.N. Kang et al., Physica C 385 (2003) 24, and references therein.
[19] W.N. Kang, H.-J. Kim, E.-M. Choi, S.-I. Lee, Science 292 (2001) 1521.
[20] M.N. Kunchur, Sung-Ik. Lee, W.N. Kang, Phys. Rev. B 68 (2003) 064516.